International Journal of Solids and Structures xxx (2010) xxx–xxx

Contents lists available at ScienceDirect

International Journal of Solids and Structures

journal homepage: www.elsevier.com/locate/ijsolstr

A theory of sound transmission through a clamped curved piezoelectric membrane connected to a negative capacitor

T. Sluka [a,b,c,*], P. Mokrý [a], H. Lissek [c]

[a] Institute of Mechatronics and Computer Engineering, Technical University of Liberec, CZ-46117 Liberec, Czech Republic
[b] Ceramics Laboratory, Swiss Federal Institute of Technology (EPFL), CH-1015 Lausanne, Switzerland
[c] Laboratory of Electromagnetics and Acoustics, Swiss Federal Institute of Technology (EPFL), CH-1015 Lausanne, Switzerland

ARTICLE INFO

Article history:
Received 10 February 2009
Received in revised form 5 April 2010
Available online xxxx

Keywords:
Piezoelectric membrane
Elasticity control
Noise shielding
Negative capacitor

ABSTRACT

An analytical calculation of the acoustic transmission loss of sound propagating through a thin cylindrically curved piezoelectric membrane, which is rigidly clamped at its straight ends, is presented. The membrane is placed inside an acoustic tube and connected to an active electric shunt circuit that behaves as a negative capacitor. A properly adjusted shunt circuit has a significant impact on the effective elastic stiffness of the piezoelectric membrane and, hence, influences the membrane acoustic reflectivity and transmission loss of sound. Such a setup represents a noise control system based on the principles of the active elasticity control of piezoelectric materials. The non-uniform radial motion of the clamped membrane and its interaction with the acoustic field and the electric shunt circuit are analyzed. The main objective of the calculations, which are based on Donnell's theory, is the determination of the effects of the membrane clamps on the flexural motion of the membrane and, therefore, effects on the acoustic transmission loss of sound. Approximative formulae for the amplitude of the membrane displacement and the acoustic transmission loss of sound are expressed as well as the resonant frequencies of the uniform mode and flexural vibration modes.

1. Introduction

Modern acoustic devices widely utilize piezoelectric elements as electro-acoustic transducers. One of the transduction concepts uses a piezoelectric cylindrically curved membrane, which is rigidly clamped at its straight ends. The principle of transduction is that the voltage-induced elongation and contraction of the membrane cause its displacement in the radial direction. The membrane interacts with a surrounding medium through its radial motion while it simultaneously interacts with an electrical circuit which is connected to the electrodes on the membrane surface.

The curved piezoelectric membranes, which are often made of polyvinylidene fluoride (PVDF), have found wide use in acoustic applications such as speakers (tweeters), headphones, microphones, hydrophones, and ultrasound generators and receivers, etc., (see Tamura et al., 1975, Lerch and Sessler, 1980). Recently, PVDF membranes have been studied as the fundamental components of noise control systems based on a method to control the effective elastic stiffness of piezoelectric elements by a shunt circuit, (see Date et al., 2000). In this method, the electric properties of a shunt circuit are manifested in the elastic and acoustic properties of the membrane, which can theoretically be enhanced to a large extent. Kodama et al. (2002) and Fukada et al. (2004) used this method to create a noise shielding system with a shunt negative capacitor[1] which increases the effective elastic stiffness of a PVDF membrane up to extreme values. The stiff membrane then acts as a noise shielding element with high acoustic reflectivity.

The principle of the noise shielding is based on simultaneous utilization of the direct and inverse piezoelectric effects. An incident acoustic pressure acting on the piezoelectric membrane induces a strain (according to Hook's law) and a voltage (by the direct piezoelectric effect). The voltage is introduced to the negative capacitor, which "pushes" the charge back to the piezoelectric membrane and causes a charge induced strain (by the inverse piezoelectric effect) with an opposite sign to the force induced strain. When the sum of capacitances of the piezoelectric membrane and the negative capacitor equals zero, the force induced strain is exactly compensated by the charge induced strain, i.e. the total strain is zero under an arbitrary incident acoustic pressure. As a result, the elastic stiffness of the membrane is effectively infinite, which also leads to an infinite value of the acoustic transmission loss.

The theoretical efficiency of these noise control systems is extraordinarily high relative to their simple technical performance. On the other hand, the systems suffer from low stability and a high

* Corresponding author: Address: Ceramics Laboratory, Swiss Federal Institute of Technology (EPFL), CH-1015 Lausanne, Switzerland. Tel.: +41 216934956.
E-mail addresses: tomas.sluka@epfl.ch (T. Sluka), pavel.mokry@tul.cz (P. Mokrý).

[1] Impedance inverter which has effectively negative capacitance (see Bogert, 1955).

0020-7683/$ - see front matter © 2010 Elsevier Ltd. All rights reserved.
doi:10.1016/j.ijsolstr.2010.04.019

sensitivity to changes in operating conditions, (see Sluka et al., 2008). One of the essential problems which hinder further development of the noise shielding systems is the insufficient understanding of the membrane dynamics. However, numerous related works have been published. Tamura et al. (1975) and Edelman and Dereggi (1976) dealt with a static analysis, and Fiorillo (1992) analyzed the resonance modes, assuming a uniform membrane displacement and neglecting the effects of membrane clamping. Mokrý et al. (2003a,b) analyzed the model of the noise shielding system with a thin piezoelectric membrane connected to the negative capacitor assuming uniform membrane motion in an acoustic field.

A more detailed theoretical analysis of coupling between the uniform mode and the flexural modes was discussed by Wang and Toda (1999) and Toda and Tosima (2000) for a curved PVDF membrane in the ultrasound frequency region. However, their model does not cover the membrane interaction with the external shunt circuit and their solution of the model is numerical. In the work by Bailo et al. (2003), simple analytical models were derived and experimentally validated to predict the structural dynamics and acoustic responses of PVDF diaphragms.

Apart from the noise control issues, non-piezoelectric thin cylindrical shells, which are clamped at their boundary, are also commonly used as mechanical structures in the space and aircraft industry, e.g. as a fuselage for missiles, aircraft or tanks. Also in this case, a deeper understanding of the dynamic response of curved membranes is desirable for design and analysis purposes.

Various approximate methods have been applied to the analysis of vibrations of stiffened non-piezoelectric part-shells in the past. Maddox et al. (1970) dealt with the theoretical and experimental frequency analysis of a cylindrically curved panel with clamped and elastic boundaries. Mead and Bardell (1986) calculated the wave propagation around a cylindrical shell. Shen and Wan (1987) applied *B*-spline functions to the flat shells, and Shen and Chuang (1990) extended this method to include stiffened shells and plates. Mustafa and Ali (1987) used a finite element method to predict the natural frequencies of stiffened and unstiffened shells and developed boundary conditions for the analysis of part-shells.

In this paper, we present an analytical calculation of the interaction between the clamped piezoelectric membrane, the one-port shunt electrical circuit, and the acoustic field while the complex flexural modes of membrane motion are taken into account. On that basis, a formula for the acoustic transmission loss of sound propagating through the membrane is derived as well as the formulae for the membrane displacement and resonant frequencies. The formulae also describe the dynamic behavior of non-piezoelectric membranes as a limit case where the piezoelectric coefficients are zero.

2. Model of a curved piezoelectric membrane

Fig. 1 shows the geometry of the acoustic tube with the clamped cylindrically curved piezoelectric membrane which is connected to the shunt electric circuit. The model was designed in order to interpret experimental measurements of the acoustic transmission loss by means of the method defined in ISO 10534-2 (1998).

We assume an infinite length and width of the acoustic tube in directions of the x and z axes, and inner height H along the y axis. The origin of the coordinate system denoted by [0,0] is attached to the bottom clamp of the membrane. This membrane has the thickness h and the radius of curvature R. The circumferential coordinate ξ is attached to the membrane surface and the symbols u_r and u_ξ denote the radial and tangential membrane displacements, respectively. Symbol V stands for the voltage on common electrodes of the membrane and the shunt circuit, and the symbols I and Z_{NC} denote the current and impedance densities per unit membrane width, respectively.

3. Acoustic field in the tube

We assume the tube is filled with air of zero heat conductivity, uniform volume density ρ_0, the static pressure p_0 and irrotational (non-turbulent) vector field of air particle velocities. Under this assumption, we can introduce the scalar acoustic potential ψ defined by its relation to the acoustic pressure $p = \rho_0 \partial\psi/(\partial t)$ and air particle velocity $\mathbf{v} = -\nabla\psi$. When we consider only the plane waves propagating in the x-direction in the tube, i.e. $\psi = \psi(t,x)$, the acoustic field is described by the wave equation:

$$\frac{1}{c^2}\frac{\partial^2\psi}{\partial t^2} = \frac{\partial^2\psi}{\partial x^2}, \tag{1}$$

where $c = \sqrt{p_0/\rho_0}$ is the phase velocity of sound in air.

The acoustic wave on the left-hand side of the tube ($x < 0$) is a sum of the incident sound wave ψ_i and the sound wave reflected from the membrane ψ_r. Similarly, ψ_t describes the wave transmitted through the membrane. Thus, one can write

$$\psi = \begin{cases} \psi_i + \psi_r & \text{for} \quad x < 0, \\ \psi_t & \text{for} \quad x > 0. \end{cases}$$

We restrict our analysis to the harmonic plane waves propagating in the x-direction inside the acoustic tube. Then the solution of Eq. (1) has a simple form

$$\psi_i = \Psi_i e^{j\omega(t-x/c)}, \quad \psi_r = \Psi_r e^{j\omega(t+x/c)}, \quad \psi_t = \Psi_t e^{j\omega(t-x/c)}. \tag{2}$$

The condition of continuity of v_x component of the air particle velocity at the membrane surface

$$v_x(x=0) = \left.\frac{\partial\psi_i}{\partial x}\right|_{x=0} + \left.\frac{\partial\psi_r}{\partial x}\right|_{x=0} = \left.\frac{\partial\psi_t}{\partial x}\right|_{x=0} \tag{3}$$

and Eq. (2) give $\Psi_r = \Psi_i - \Psi_t$ and the acoustic pressure gradient δp between the opposite sides of the membrane (i.e. the pressure difference divided by membrane thickness h) is then equal to

$$\delta p = \frac{\rho_0}{h}\left(\frac{\partial\psi_i}{\partial t} + \frac{\partial\psi_r}{\partial t} - \frac{\partial\psi_t}{\partial t}\right)\Bigg|_{x=0} = 2j\omega\frac{\rho_0}{h}(\Psi_i - \Psi_t)e^{j\omega t}. \tag{4}$$

This equation represents the force interaction between the acoustic field and the membrane.

4. Dynamics of the membrane motion

In this section we analyze the dynamics of the cylindrically curved membrane under conditions, which are consistent with most of the experimental situations, where (i) the membrane is made of an elastically isotropic material, (ii) the membrane thickness is much smaller than the radius of membrane curvature ($h \ll R$), and (iii) the membrane displacements are smaller than the membrane thickness ($|u_r| \ll h$). Since the equations governing the membrane motion can be expressed in terms of u_r and u_ξ, we consider purely geometrical relationship between them according to Donnell's shallow shell theory, (see, e.g., Vinson, 1992). Under this assumption, the longitudinal strain e_ξ and the flexural strain χ_ξ of the membrane in the ξ-direction are given as follows:

$$e_\xi = \frac{\partial u_\xi}{\partial\xi} - \frac{u_r}{R}, \quad \chi_\xi = \frac{\partial^2 u_r}{\partial\xi^2}. \tag{5}$$

All remaining strain components are zero due to the model symmetry. Further, we consider a single nonzero component $d_{r\xi}$ of the tensor of piezoelectric coefficients and the corresponding equation of state

Please cite this article in press as: Sluka, T., et al. A theory of sound transmission through a clamped curved piezoelectric membrane connected to a negative capacitor. Int. J. Solids Struct. (2010), doi:10.1016/j.ijsolstr.2010.04.019

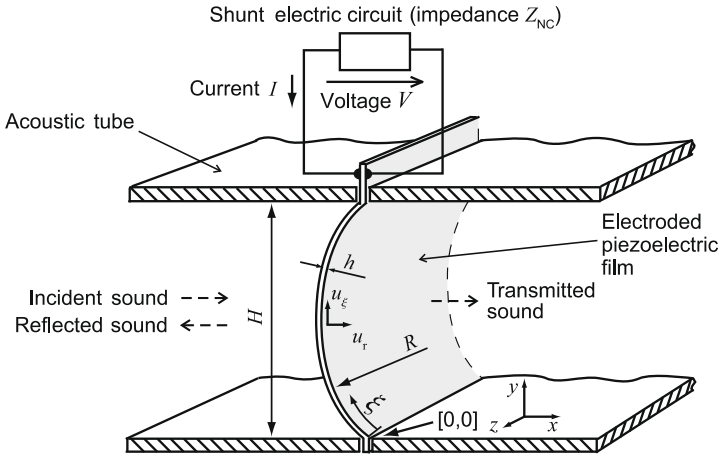

Fig. 1. Geometry of the curved piezoelectric membrane model for the calculation of the acoustic transmission loss of sound. A cylindrically curved membrane of a thickness h and of the radius of curvature R is clamped at its straight edges between two parts of the acoustic tube of an inner height H. An incident sound wave strikes the membrane from the left side of the tube. The incident sound wave is partially reflected and partially transmitted making the membrane vibrate. Displacement of the membrane in the radial and tangential directions are denoted by symbols u_r and u_ξ, respectively. The membrane electrodes are shunted by the external circuit of the impedance Z_{NC}, which has a strong impact on the transmission of sound due to the piezoelectric effects.

$$\tau_\xi = c^E_{\xi\xi}(e_\xi - d_{r\xi}E_r), \tag{6}$$

where τ_ξ is the mechanical stress along the ξ-coordinate, $c^E_{\xi\xi}$ is the component of the elastic stiffness tensor, which couples the stress and strain along the ξ-coordinate, and $d_{r\xi}$ is the piezoelectric coefficient coupling the stress τ_ξ with the electric field E_r perpendicular to the membrane surface. The moment of bending forces (per unit membrane thickness and width) is equal to

$$M_\xi = m_\xi \chi_\xi / h, \tag{7}$$

where the flexural compliance $m_\xi = c^E_{\xi\xi}h^3/12$ is calculated for the rectangular cross section of the membrane of a unit width and the thickness h.

At this moment, it is possible to obtain a system of partial differential equations governing the membrane motion. From the equilibrium of forces and moments shown in Fig. 2, it directly follows that

$$\frac{\partial \tau_\xi}{\partial \xi} = \rho \frac{\partial^2 u_\xi}{\partial t^2}, \quad \delta p + \frac{\tau_\xi}{R} - \frac{\partial N_\xi}{\partial \xi} = \rho \frac{\partial^2 u_r}{\partial t^2}, \quad \frac{\partial M_\xi}{\partial \xi} - N_\xi = 0, \tag{8}$$

where N_ξ is the normal stress in the membrane and the moment of inertia of the membrane is neglected. The straightforward substitution of Eqs. (5)–(7) into Eq. (8), and the elimination of N_ξ by expressing it from the third and substituting it into the second of Eq. (8) yield the system of equations

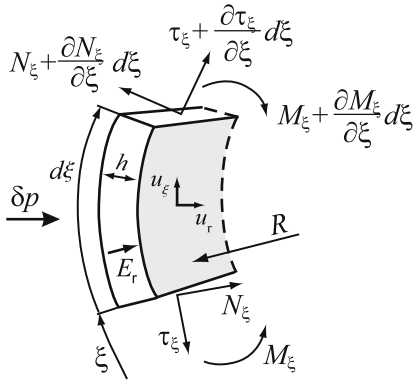

Fig. 2. Forces and bending moments per unit length acting on the infinitesimal element of the cylindrically curved membrane.

$$\frac{\partial^2 u_\xi}{\partial \xi^2} - \frac{1}{R}\frac{\partial u_r}{\partial \xi} = \frac{\rho}{c^E_{\xi\xi}}\frac{\partial^2 u_\xi}{\partial t^2}, \tag{9a}$$

$$-\frac{h^2}{12}\frac{\partial^4 u_r}{\partial \xi^4} + \frac{1}{R}\frac{\partial u_\xi}{\partial \xi} - \frac{u_r}{R^2} + \frac{\delta p}{c^E_{\xi\xi}} - \frac{d_{r\xi}}{R}E_r = \frac{\rho}{c^E_{\xi\xi}}\frac{\partial^2 u_r}{\partial t^2}. \tag{9b}$$

In addition, it is necessary to append Eqs. (9) with boundary conditions

$$u_r(0) = 0, \quad u_\xi(0) = 0, \quad \left.\frac{\partial u_r}{\partial \xi}\right|_{\xi=0} = 0, \tag{10a}$$

$$u_r(H) = 0, \quad u_\xi(H) = 0, \quad \left.\frac{\partial u_r}{\partial \xi}\right|_{\xi=H} = 0, \tag{10b}$$

which correspond to zero membrane displacement and flexion at both clamped edges of the membrane.

Since we assume the linear system in a steady state forced by harmonic acoustic pressure fluctuations with the angular frequency ω, we can consider the harmonic time dependence of state quantities of the system:

$$E_r = E e^{j\omega t}, \quad \delta p = \delta P e^{j\omega t}, \quad u_\xi = U_\xi(\xi)e^{j\omega t}, \quad u_r = U_r(\xi)e^{j\omega t}. \tag{11}$$

Then, it is possible to reduce Eqs. (9) to the form

$$\mathfrak{D}(U_\xi) = 0, \tag{12a}$$

$$\mathfrak{D}(U_r) = \frac{1}{c^E_{\xi\xi}}\delta P - \frac{d_{r\xi}}{R}E, \tag{12b}$$

where $U_\xi = U_\xi(\xi)$, $U_r = U_r(\xi)$ are the amplitudes of the tangential and radial membrane displacement, respectively, and $\mathfrak{D}$ is the differential operator

$$\mathfrak{D} = \frac{h^2}{12\Omega^2}\frac{\partial^6}{\partial \xi^6} + \frac{h^2}{12}\frac{\partial^4}{\partial \xi^4} - \frac{\partial^2}{\partial \xi^2} + \left(\frac{1}{R^2} - \Omega^2\right), \tag{13}$$

where $\Omega^2 = \rho\omega^2/c^E_{\xi\xi}$.

We solve the boundary value problem given by Eqs. (10) and (12). As usual, the solution of the non-homogenous Eq. (12b) is found as a sum of the solution of the homogenous equation and the particular integral, i.e.

$$U_r(\xi) = U_h(\xi) + U_p. \tag{14}$$

Eq. (12a) is homogeneous and, hence, $U_\xi(\xi)$ is directly its homogeneous solution.

Please cite this article in press as: Sluka, T., et al. A theory of sound transmission through a clamped curved piezoelectric membrane connected to a negative capacitor. Int. J. Solids Struct. (2010), doi:10.1016/j.ijsolstr.2010.04.019

Homogeneous solution. The differential operator $\mathfrak{D}$ given by Eq. (13) is of the sixth order, however only the partial derivatives of the even order are present. In that case, there exists a trick according to Cardano (1545), which is based on a convenient form of the solution of the homogenous equation

$$U_\xi(\xi) \propto U_h(\xi) \propto e^{\pm j\xi\sqrt{\lambda+\Omega^2/3}}. \tag{15}$$

Substituting Eq. (15) into the homogeneous Eqs. (12a) or (12b), we get the characteristic polynomial of the form:

$$\lambda^3 - 3p\lambda - q = 0, \tag{16}$$

where

$$p = \Omega^2\left(\frac{4}{h^2}+\frac{\Omega^2}{9}\right) \approx \frac{4\Omega^2}{h^2}, \tag{17a}$$

$$q = \frac{2\Omega^6}{27}+\frac{\Omega^2}{h^2}\left(\frac{12}{R^2}-8\Omega^2\right) \approx \frac{\Omega^2}{h^2}\left(\frac{12}{R^2}-8\Omega^2\right). \tag{17b}$$

The approximations in Eqs. (17) are valid if $h^2 \ll \Omega^{-2}$, which is a widely acceptable assumption in the realistic experimental situations. However, in the case of Eq. (17b) the approximation is inaccurate in a small frequency region in the vicinity of $\omega = \sqrt{3/2}\,\omega_r$, where $\omega_r = 1/R\sqrt{|c^E_{\xi\xi}|/\rho}$ is the well known resonant frequency of the uniform membrane motion. This inaccuracy becomes negligible as soon as the complex character of $c^E_{\xi\xi}$ is taken into account.

The roots of the characteristic Eq. (16) are found as follows:

$$\lambda_1 = \frac{p}{\sqrt[3]{\mathscr{y}}}+\sqrt[3]{\mathscr{y}},$$

$$\lambda_2 = -\frac{\left(1+j\sqrt{3}\right)p}{\sqrt[3]{8\mathscr{y}}}-\left(1-j\sqrt{3}\right)\sqrt[3]{\mathscr{y}/8},$$

$$\lambda_3 = -\frac{\left(1-j\sqrt{3}\right)p}{\sqrt[3]{8\mathscr{y}}}-\left(1+j\sqrt{3}\right)\sqrt[3]{\mathscr{y}/8},$$

where $\mathscr{y} = 1/2\,(q+\sqrt{q^2-4p^3})$. Hence, the homogeneous solution of Eqs. (12) is given by

$$U_\xi(\xi) = \sum_{\mu=1}^{3}\frac{\Lambda_\mu}{R\left(\Lambda_\mu^2-\Omega^2\right)}\left(U_H^{(2\mu-1)}\sin\Lambda_\mu\xi - U_H^{(2\mu)}\cos\Lambda_\mu\xi\right), \tag{18a}$$

$$U_h(\xi) = \sum_{\mu=1}^{3}\left(U_H^{(2\mu-1)}\cos\Lambda_\mu\xi - U_H^{(2\mu)}\sin\Lambda_\mu\xi\right), \tag{18b}$$

where $\Lambda_\mu = \sqrt{\lambda_\mu+\Omega^2/3}$, and $U_H^{(2\mu-1)}$ and $U_H^{(2\mu)}$ are unknown parameters for $\mu = 1,2,3$. One can find the approximations of Λ_μ for all aforementioned assumptions as follows:

$$\Lambda_1 \approx \sqrt{12\,\Omega/h}, \quad \Lambda_2 \approx j\Lambda_1,$$

$$\Lambda_3 \approx \sqrt{-(-2)^{1/3}M+\left(\frac{1}{3}+\frac{2(-2)^{2/3}}{h^2M}\right)\Omega^2}, \tag{19}$$

where

$$M = \sqrt[3]{\frac{\Omega^2}{h^2}\left(\frac{3}{R^2}-2\Omega^2\right)+\frac{\Omega^2}{h^2}\sqrt{\frac{9}{R^4}-\frac{16\Omega^2}{h^2}}}.$$

Particular solution. Eq. (12a) is homogeneous and therefore its particular integral is zero. Substitution of Eqs. (4) into Eq. (12b) gives the particular solution in the form

$$U_p = \frac{R}{\rho R^2\omega^2 - c^E_{\xi\xi\xi}}\left[\frac{2j\omega\rho_0 R}{h}(\Psi_t-\Psi_i)+c^E_{\xi\xi}d_{r\xi}E\right]. \tag{20}$$

Boundary value problem. The unknown coefficients $U_H^{(\mu)}$ in Eqs. (18) are determined by substituting Eqs. (11), in which $U_r(\xi)$ is given by Eq. (14), to the boundary conditions (10). Then we obtain

$$U_\xi(0) = 0, \quad U_h(0)+U_p = 0, \quad \left.\frac{\partial U_h(\xi)}{\partial\xi}\right|_{\xi=0} = 0, \tag{21a}$$

$$U_\xi(H) = 0, \quad U_h(H)+U_p = 0, \quad \left.\frac{\partial U_h(\xi)}{\partial\xi}\right|_{\xi=H} = 0. \tag{21b}$$

Substituting $U_\xi(\xi)$ and $U_h(\xi)$ from Eqs. (18) and U_p from Eq. (20) to Eq. (21) yields the system of the linear algebraic equations **A**.**x** = **b**, where

$$\mathbf{A} = \begin{pmatrix} 0 & G_1 & 0 & G_2 & 0 & G_3 \\ 1 & 0 & 1 & 0 & 1 & 0 \\ 0 & \Lambda_1 & 0 & \Lambda_2 & 0 & \Lambda_3 \\ -G_1\sin H\Lambda_1 & G_1\cos H\Lambda_1 & -G_2\sin H\Lambda_2 & G_2\cos H\Lambda_2 & -G_3\sin H\Lambda_3 & G_3\cos H\Lambda_3 \\ \cos H\Lambda_1 & \sin H\Lambda_1 & \cos H\Lambda_2 & \sin H\Lambda_2 & \cos H\Lambda_3 & \sin H\Lambda_3 \\ -\Lambda_1\sin H\Lambda_1 & \Lambda_1\cos H\Lambda_1 & -\Lambda_2\sin H\Lambda_2 & \Lambda_2\cos H\Lambda_2 & -\Lambda_3\sin H\Lambda_3 & \Lambda_3\cos H\Lambda_3 \end{pmatrix},$$

x = $(U_H^{(1)},U_H^{(2)},U_H^{(3)},U_H^{(4)},U_H^{(5)},U_H^{(6)})^T$, and **b** = $(0,-1,0,0,-1,0)^T U_p$. In these equations $G_\mu = \Lambda_\mu(\Lambda_\mu^2-\Omega^2)/R$ for $\mu = 1,2,3$.

The system of equations **A**.**x** = **b** has a solution in the form

$$U_H^{(\nu)} = K_{UH}^{(\nu)}U_p, \tag{22}$$

where $\nu = 1,2,\ldots,6$ and

$$K_{UH}^{(1)} = \frac{G_2\Lambda_3-G_3\Lambda_2}{G_3\Lambda_2-G_2\Lambda_3+\left[(G_1\Lambda_3-G_3\Lambda_1)\cot\frac{H\Lambda_2}{2}+(G_2\Lambda_1-G_1\Lambda_2)\cot\frac{H\Lambda_3}{2}\right]\tan\frac{H\Lambda_1}{2}},$$

$$K_{UH}^{(2)} = \frac{G_2\Lambda_3-G_3\Lambda_2}{(G_3\Lambda_2-G_2\Lambda_3)\cot\frac{H\Lambda_1}{2}+(G_1\Lambda_3-G_3\Lambda_1)\cot\frac{H\Lambda_2}{2}+(G_2\Lambda_1-G_1\Lambda_2)\cot\frac{H\Lambda_3}{2}},$$

$$K_{UH}^{(3)} = \frac{G_3\Lambda_1-G_1\Lambda_3}{G_1\Lambda_3-G_3\Lambda_1+\left[(G_3\Lambda_2-G_2\Lambda_3)\cot\frac{H\Lambda_1}{2}+(G_2\Lambda_1-G_1\Lambda_2)\cot\frac{H\Lambda_3}{2}\right]\tan\frac{H\Lambda_2}{2}},$$

$$K_{UH}^{(4)} = \frac{G_3\Lambda_1-G_1\Lambda_3}{(G_3\Lambda_2-G_2\Lambda_3)\cot\frac{H\Lambda_1}{2}+(G_1\Lambda_3-G_3\Lambda_1)\cot\frac{H\Lambda_2}{2}+(G_2\Lambda_1-G_1\Lambda_2)\cot\frac{H\Lambda_3}{2}},$$

$$K_{UH}^{(5)} = \frac{G_1\Lambda_2-G_2\Lambda_1}{G_2\Lambda_1-G_1\Lambda_2+\left[(G_3\Lambda_2-G_2\Lambda_3)\cot\frac{H\Lambda_1}{2}+(G_1\Lambda_3-G_3\Lambda_1)\cot\frac{H\Lambda_2}{2}\right]\tan\frac{H\Lambda_3}{2}},$$

$$K_{UH}^{(6)} = \frac{G_1\Lambda_2-G_2\Lambda_1}{(G_3\Lambda_2-G_2\Lambda_3)\cot\frac{H\Lambda_1}{2}+(G_1\Lambda_3-G_3\Lambda_1)\cot\frac{H\Lambda_2}{2}+(G_2\Lambda_1-G_1\Lambda_2)\cot\frac{H\Lambda_3}{2}}.$$

One obtains the solution of the amplitude of tangential displacement $U_\xi(\xi)$ by substituting $U_H^{(\mu)}$ given by Eq. (22) into Eq. (18a) and amplitude of radial displacement $U_r(\xi)$ by substituting Eq. (22) into Eq. (14) where $U_h(\xi)$ and U_p are given by Eqs. (18b) and (20), respectively. After the substitution, formulae (18a) and (14) represent the membrane displacement. However, they are still functions of the independent complex amplitudes of the external electric field E and the acoustic potentials Ψ_i and Ψ_t. Therefore, it is necessary to incorporate interactions of the membrane with the acoustic field and the negative capacitor which eliminate the unknown variables.

5. Membrane interaction with the shunt circuit

The piezoelectric membrane is connected to the linear electric shunt circuit, which is characterized by the density (per unit membrane width) of its electrical impedance

$$Z_{NC} = -\frac{Eh}{I}. \tag{23}$$

The current I flows from the circuit and $E = V/h$ with the orientation of V as introduced in Fig. 1. The current density I is calculated as a time derivative of the free charge integrated over the membrane surface of an unit membrane width. Since the free charge density is equal to the component of the electrical displacement $D(\xi)$, which is perpendicular to the membrane surface, one can calculate the current density I from the equation

Please cite this article in press as: Sluka, T., et al. A theory of sound transmission through a clamped curved piezoelectric membrane connected to a negative capacitor. Int. J. Solids Struct. (2010), doi:10.1016/j.ijsolstr.2010.04.019

$$I=\int_0^H j\omega D(\xi)d\xi,\quad \text{where } D(\xi)=\varepsilon_0\varepsilon_{rr}^e E+c_{\xi\xi}^E d_{r\xi}\left(\frac{\partial U_\xi(\xi)}{\partial\xi}-\frac{U_r(\xi)}{R}\right). \tag{24}$$

The expression in parenthesis on the right hand side of Eq. (24) is the elastic strain along the membrane surface which follows from the strain e_ξ defined by Eq. (5). The symbol ε_{rr}^e denotes the relative permittivity of the membrane material under a constant strain.

Combining Eqs. (23) and (24) gives

$$\int_0^H\left(\frac{\partial U_\xi(\xi)}{\partial\xi}-\frac{U_r(\xi)}{R}\right)d\xi=\frac{Eh}{j\omega c_{\xi\xi}^E d_{r\xi}}\left(\frac{1}{Z_{NC}}+\frac{1}{Z_s}\right), \tag{25}$$

where $Z_s=-jh/(\omega H\varepsilon_0\varepsilon_{rr}^e)$ is the density of the membrane electrical impedance per unit width. Eq. (25) couples the membrane motion with the impedance of the shunt circuit.

6. Membrane interaction with an acoustic field

The interaction of the membrane with the acoustic field is introduced by Eq. (4) and by the fact that the air particle velocity and membrane velocity in the x-direction (v_x) at the membrane surface (x = 0) are equal.

Since we restricted our analysis to the transmission of planar waves, only the interaction between the plane wave and the uniform part of the membrane radial displacement is taken into account. It means that also v_x is equal to the uniform part of the membrane velocity according to following relation

$$v_x(x=0)=\frac{1}{H}\int_0^H\frac{\partial u_r(\xi)}{\partial t}d\xi\quad\Rightarrow\quad\frac{j\omega\Psi_t}{c}=\frac{1}{H}\int_0^H j\omega U_r(\xi)d\xi. \tag{26}$$

Eq. (26) couples the uniform part of the membrane displacement $U_r(\xi)$ and the acoustic potential Ψ_t of the transmitted sound wave.

7. Amplitude of the membrane displacement

Amplitudes of membrane displacement expressed as functions of Ψ_i are obtained when Ψ_t and E are derived from the conditions given by Eqs. (25) and (26). They can be expressed in a convenient form using coefficients $K_{\Psi t}$ and K_E as follows:

$$\Psi_t=K_{\Psi t}\Psi_i$$

$$\text{where } K_{\Psi t}=\left(1+j\frac{h}{\Im}\frac{R^2\rho\omega^2-c_{\xi\xi}^E+\left[R^2\rho\omega^2-c_{\xi\xi}^E(1+\kappa^2\Im)\right]Z_{NC}/Z_s}{2c\rho_0R^2\omega(1+Z_{NC}/Z_s)}\right)^{-1}, \tag{27a}$$

$$E=K_E\Psi_i$$

$$\text{where } K_E=\frac{\kappa^2}{d_{r\xi}cR}\left[1+\frac{Z_s}{Z_{NC}}+j\frac{h}{\Im}\frac{R^2\rho\omega^2-c_{\xi\xi}^E+\left[R^2\rho\omega^2-c_{\xi\xi}^E(1+\kappa^2\Im)\right]Z_{NC}/Z_s}{2c\rho_0R^2\omega Z_{NC}/Z_s}\right]^{-1}. \tag{27b}$$

Here

$$\Im\approx 1-\Omega^2\left[\frac{H}{4}\Lambda_1\Lambda_3^2\left(\cot\frac{H\Lambda_1}{2}+\coth\frac{H\Lambda_1}{2}\right)+\Omega^2-\Lambda_3^2\right]^{-1} \tag{28}$$

is a dimensionless function of frequency and $\kappa^2=c_{\xi\xi}^E d_{r\xi}^2/(\varepsilon_0\varepsilon_{rr}^e)$ is the electromechanical coupling factor of the piezoelectric material. Now we can write U_p in a simple form

$$U_p=\frac{R}{\rho R^2\omega^2-c_{\xi\xi}^E}\left[\frac{2j\omega\rho_0R}{h}(K_{\Psi t}-1)+c_{\xi\xi}^E d_{r\xi}K_E\right]\Psi_i \tag{29}$$

and then, using Eq. (22), also formulae for the amplitudes of the membrane displacement

$$U_\xi(\xi)=\frac{R}{\rho R^2\omega^2-c_{\xi\xi}^E}\left[\sum_{\mu=1}^3\frac{\Lambda_\mu}{R\left(\Lambda_\mu^2-\Omega^2\right)}\left(K_{UH}^{(2\mu-1)}\sin\Lambda_\mu\xi-K_{UH}^{(2\mu)}\cos\Lambda_\mu\xi\right)\right]\times\left[\frac{2j\omega\rho_0R}{h}(K_{\Psi t}-1)+c_{\xi\xi}^E d_{r\xi}K_E\right]\Psi_i, \tag{30a}$$

$$U_r(\xi)=\frac{R}{\rho R^2\omega^2-c_{\xi\xi}^E}\left[1+\sum_{\mu=1}^3\left(K_{UH}^{(2\mu-1)}\cos\Lambda_\mu\xi-K_{UH}^{(2\mu)}\sin\Lambda_\mu\xi\right)\right]\times\left[\frac{2j\omega\rho_0R}{h}(K_{\Psi t}-1)+c_{\xi\xi}^E d_{r\xi}K_E\right]\Psi_i. \tag{30b}$$

8. Acoustic transmission loss through the membrane

The transmission loss is defined as the fraction of Ψ_t and Ψ_i as follows:

$$TL=20\log_{10}\left|\frac{\Psi_i}{\Psi_t}\right|. \tag{31}$$

Straightforward substitution of Eq. (27a) into Eq. (31) gives

$$TL=20\log_{10}\left|1+j\frac{h}{\Im}\frac{R^2\rho\omega^2-c_{\xi\xi}^E+\left[R^2\rho\omega^2-c_{\xi\xi}^E(1+\kappa^2\Im)\right]Z_{NC}/Z_s}{2c\rho_0R^2\omega(1+Z_{NC}/Z_s)}\right|. \tag{32}$$

In order to understand this expression, it is convenient to introduce a complex parameter $\omega_r^*=(1/R)\sqrt{c_{\xi\xi}^E/\rho}$, which, in absolute value, is equal to the resonant frequency of the uniform mode of membrane motion. Using the parameter ω_r^*, one obtains a compact form of Eq. (32) as follows:

$$TL=20\log_{10}\left|1+j\frac{h\rho}{2c\rho_0}\left(\frac{1}{\Im}\frac{\omega^2-\omega_r^{*2}}{\omega}-\kappa^2\frac{Z_{NC}}{Z_{NC}+Z_s}\frac{\omega_r^{*2}}{\omega}\right)\right|. \tag{33}$$

In the above equation it is clearly seen that when the impedances of the electric shunt circuit Z_{NC} and the piezoelectric membrane Z_s meet condition $Z_{NC}=-Z_s$, the acoustic transmission loss through the membrane is tending to infinity.

Another view on Eq. (33) can be obtained by introducing the formulae for acoustic impedances of air $z_a=c\rho_o$ and the membrane $z_m=(1/\Im)(z_m^{(m)}+z_m^{(e)})$, where $z_m^{(m)}=j\omega h\rho$ and $z_m^{(e)}=-jhc_{\xi\xi}^E/(R^2\omega)$ are contributions to the acoustic impedance of the membrane controlled by its mass and stiffness, respectively. Finally, if we introduce the capacitance of the membrane $C_s^e=\varepsilon_0\varepsilon_{rr}^e H/h$ and the capacitance of the external circuit C_{NC}, we can write the density of the electrical impedance of the membrane $Z_s=-j/(\omega C_s^e)$ and the shunt circuit $Z_{NC}=-j/(\omega C_{NC})$. Now, using the expression $\Delta C_e=C_s^e+C_{NC}$, the formula for the transmission loss is as follows:

$$TL=20\log_{10}\left|1+\frac{z_m}{2z_a}+\kappa^2\frac{z_m^{(e)}}{2z_a}\frac{C_s^e}{\Delta C_e}\right|. \tag{34}$$

Again it is seen that matching the electric shunt circuit capacitance and the minus of the piezoelectric membrane capacitance, i.e. $\Delta C_e\approx 0$, results in the increase in the values of the acoustic transmission loss TL.

Numerical results. Detailed verification of the model by comparison with experimental results exceeds the scope of this article, which primarily presents a derivation of the analytical solution. However, we discuss several concrete cases in this section. The thorough model verification will be published by Sluka et al..

In order to obtain specific numerical results we use well known formulae for the frequency dependence of relative permittivity $\varepsilon_{rr}^e=\varepsilon_\infty^e+(\varepsilon_s^e-\varepsilon_\infty^e)/[1+(j\omega\mathscr{T})^{b_1}]^{b_2}$ of polymer dielectrics, (see

Please cite this article in press as: Sluka, T., et al. A theory of sound transmission through a clamped curved piezoelectric membrane connected to a negative capacitor. Int. J. Solids Struct. (2010), doi:10.1016/j.ijsolstr.2010.04.019

Herbert et al., 1998), and the elastic stiffness $c^E_{\xi\xi} = Re(c^E_{\xi\xi})(1 + j\tan\delta)$. Symbols ε^e_s and ε^e_∞ represent the empirically determined limits of the relative permittivities for zero and infinity frequencies, respectively. Symbols b_1 and b_2 are the dimensionless constants and $\tan\delta$ is the mechanical loss factor of the membrane material. The shunt circuit adopted in our analysis is a negative capacitor realized with use of the ideal operational amplifier shown in the inset of Fig. 3(b). Date et al. (2000) and Mokrý et al. (2003a) showed that the complex input capacitance of such a circuit is equal to $C_{NC} = -R_2C_0/[R_1(1 + j\omega C_0R_0)]$. The values of circuit parameters R_2, R_1, C_0, R_0 of the negative capacitor are chosen in a way to achieve the desired matching of the membrane and circuit capacitances at a given frequency ω_0, i.e. $\Delta C_e(\omega_0) = 0$. Therefore, the values are chosen as follows: $C_0 = Re[C^e_s(\omega_0)]$, $R_0 = Im[j\omega_0 C^e_s(\omega_0)]^{-1}$ and ratio $\alpha = R_2/R_1 = 1$ if not introduced otherwise in Fig. 3(b).

Fig. 3 shows the essential features of the derived formula for the transmission loss of sound given by Eq. (34). The graphs are generated with a material and geometric parameters introduced primarily inside the particular graphs. Other parameters are listed in Table 1. Graphs in Fig. 3(b) and (d) basically simulate measurements published by Fukada et al. (2004) while no fitting of the model parameters was needed to achieve relatively good agreement with the Fukada's measurements.

Effects of following variables on the transmission loss of sound are shown: (a) membrane radius R, (b) ratio of the resistances $\alpha = R_2/R_1$, (c) mechanical loss factor $\tan\delta$ of the membrane, and (d) the frequency ω_0 where $\Delta C_e(\omega_0) = 0$.

In Figs. 3(a) and (c) we show *TL* in a questionable range up to 20 kHz while the plane wave assumption is generally limited to frequencies $f < c/H$. On the other hand, we can assume incident plane waves even at higher frequencies where only the reflected and transmitted waves carry contribution from the sound interaction with flexural modes of the membrane motion. However, we assume and we have also confirmed by a more complex numerical model (unpublished), that the non-planar waves do not significantly contribute to the total acoustic pressure and the membrane motion. Therefore, *TL* is mainly governed by the plane waves and we present results up to $f = 20$ kHz.

In Figs. 3(a), (c) and (d) the minimum value of *TL* (the apex of the generally "V"-shape curve) corresponds to the resonant frequency ω_r of the uniform vibration mode of the membrane, which is often referred to as a "breath mode". In Fig. 3(b), this resonance is out of the plot range. Fig. 3(a) shows that the breath mode resonance can be largely controlled by the membrane curvature.

In all Fig. 3, the effect of the membrane interaction with the negative capacitor is exhibited as a huge increase of *TL* at ω_0 which represents the main point of interest in the noise control system design.

Fig. 3(b) shows the biggest drawback of the method, which is the high sensitivity of membrane *TL* on the fluctuation of the system properties, (see also Sluka et al., 2008). One can see that even a slight mistuning of the circuit, i.e. when $\alpha \neq 1$, leads to significant drop of *TL* around ω_0. Moreover, when $0 < \alpha < 1$ the system becomes instable, (see Date et al., 2000).

The effect of the membrane clamps on *TL* is seen mostly in Fig. 3(c). The repetitive small sharp peaks on the solid curve originate from the coupling between the flexural and uniform modes of the membrane motion. Both modes cause elongation and contraction of the membrane which mediates their interaction, i.e. the membrane elongation by the flexural mode limits the average membrane displacement in the radial direction and vice versa. One

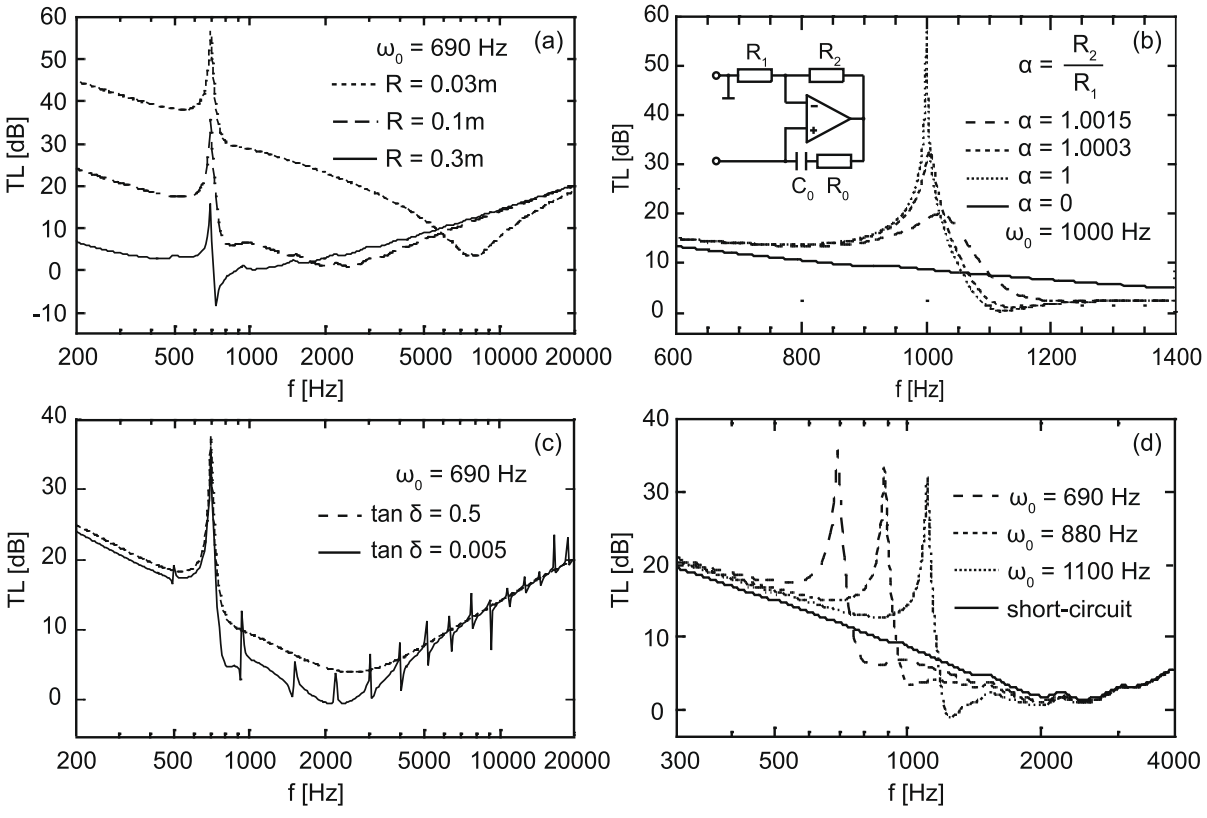

Fig. 3. The frequency dependence of the acoustic transmission loss *TL* of sound through the cylindrically curved piezoelectric membrane connected to the shunt electric circuit shown in the inset of Fig. (b). The curves are obtained using Eq. (34). Effects of following parameters are shown: (a) membrane radius R, (b) ratio of the resistances R_2/R_1, (c) mechanical loss factor $\tan\delta$ of the membrane, and (d) the frequency ω_0 where the transmission loss reaches maximum. The peak value of *TL* at the frequency ω_0 is achieved by the action of shunt electric circuit, which is utilized in the noise control systems.

Please cite this article in press as: Sluka, T., et al. A theory of sound transmission through a clamped curved piezoelectric membrane connected to a negative capacitor. Int. J. Solids Struct. (2010), doi:10.1016/j.ijsolstr.2010.04.019

Table 1
Geometrical and material parameters of the model.

Geometry	Mechanical properties	Dielectric properties	Air properties
		$\varepsilon^e_\infty = 3$	
h = 40 μm	ρ = 1700 kg/m^3	$\varepsilon^e_s = 40$	ρ_0 = 1.24 kg/m^3
R = 0.1 m	$Re(c^E_{\xi\xi}) = 3.73\,10^9$ N/m^2	$\mathscr{T} = 10^{-7}$ s	c = 343 m/s
H = 0.04 m	tanδ = 0.1	b_1 = 0.5	
		b_2 = 1	
	$d_{r\xi}$ = 10^{-11}C/N		

can see that this effect becomes obvious only when tanδ is very small. However, also the curves in Fig. 3(a) and (d), where tanδ = 0.1, show strongly damped repetitive peaks induced by flexural resonance.

Origins of the large peaks of *TL* at ω_0 induced by the action of the negative capacitor and the peaks induced by the flexural motion are basically independent. The flexural modes cause the same effect on *TL* also when the membrane is non-piezoelectric (to be published by Sluka et al.). On the other hand, the flexural resonances are projected also into the electric impedance of the piezoelectric membrane. Therefore, since the system is strongly sensitive to mismatch between the impedances of the membrane and negative capacitor, the flexural resonances represent significant unwanted disturbance. On that account, the next section analyzes the membrane flexural resonant frequencies.

9. Effect of the membrane clamps on a transmission loss of sound

A straightforward analysis of Eqs. (32) and (28) reveals that all effects introduced by the flexural modes of membrane motion on the transmission loss *TL* originate from the term $\mathfrak{S}$. To thoroughly analyze the approximative expression for $\mathfrak{S}$ let us have a look at the terms Λ_1, Λ_2, and Λ_3 given by Eq. (19). One can find that $|\Lambda_3^2|/|\Lambda_1^2| \sim h/R \ll 1$. Then the function $\mathfrak{S}$ is mainly controlled by the term in the denominator, which is proportional to Λ_1. With an increase in the frequency ω, the values of the function $\mathfrak{S}$ periodically "oscillate" around the mean value of $\mathfrak{S} \approx 1 + (1/H)\sqrt{12h/\Omega} \approx 1$. The "oscillations" are controlled by the term $\cot(H\Lambda_1/2) + \coth(H\Lambda_1/2)$, which is approximately equal to $\cot(H\Lambda_1/2) + 1$ for small h. Then the function $\mathfrak{S}$ reaches extreme values, when $\cot(H\Lambda_1/2) + 1$ approaches zero. Therefore, we find the significant frequencies by solving the equation: $\cot(H\Lambda_1/2) + 1 = 0$. Its solution is

$$\omega^*_{rf,n} = \frac{h}{8\sqrt{3}H^2}\sqrt{\frac{c^E_{\xi\xi}}{\rho}}(\pi + 2n\pi)^2, \quad n = 1, 2, 3\ldots \tag{35}$$

Here $\omega^*_{rf,n}$ are the complex parameters with absolute values corresponding to the resonant frequencies of membrane flexural modes.

10. Summary

The formula (34) represents the result of our theoretical analysis of the acoustic transmission loss of sound propagating through the clamped cylindrically curved piezoelectric membrane, which is connected to the electric shunt circuit with a negative capacitance. From this formula, we have derived the parameters $\omega^*_r = (1/R)\sqrt{c^E_{\xi\xi}/\rho}$ and $\omega^*_{rf,n}$ [see Eq. (35)], which in absolute values represent the resonant frequencies of the uniform and flexural modes of the membrane motion, respectively. In addition, results given by Eqs. (30) represent the amplitudes of radial and tangential displacement of the membrane motion.

Fig. 3 shows that within our model, we are able to reproduce several features of the frequency dependencies of the acoustic transmission loss of sound, which are present in the results of acoustic tube measurements, cf. Kodama et al. (2002) and Fukada et al. (2004): First, the generally "V"-shape of the frequency dependence of the acoustic transmission loss of sound, where the apex of the curve corresponds to the resonant frequency of the uniform vibration mode $\omega_r = (1/R)\sqrt{Y/\rho}$, is shown. In the frequency range below and above ω_r the values of *TL* are controlled by the stiffness and mass density of the membrane, respectively. Second, the peak values of the *TL* at the frequency ω_0 are achieved by the action of the connected shunt electric circuit with a negative capacitance. It is seen that using the effect of the shunt circuit, one can enhance the acoustic transmission loss of sound by additional 20–60 dB. Therefore, this effect is profitably used in the noise control systems. It is known that it is possible to broaden the band-width of this peak by use of the circuit with the distributed relaxation times, but such an analysis goes beyond the scope of this article. Third, the effect of the flexural vibration modes on the acoustic transmission loss of sound is shown.

All in all, the detailed study of the sound transmission through the cylindrically curved piezoelectric membrane presented in this article can be used for the further analysis of the sensitivity and stability of noise control systems, which are based on the method of active elasticity control of piezoelectric materials.

Acknowledgment

Authors acknowledge the support of the Czech Science Foundation Project No.: GACR 101/08/1279.

References

Bailo, K., Brei, D., Grosh, K., 2003. Investigation of curved polymeric piezoelectric active diaphragms. Journal of Vibration and Acoustics-Transactions of the Asme 125 (2), 145–154.
Bogert, B.P., 1955. Some gyrator and impedance inverter circuits. In: Proceedings of the IRE, vol. 43. pp. 793–796.
Cardano, G., 1545. Ars Magna or The Rules of Algebra. Dover Publications. 1993.
Date, M., Kutani, M., Sakai, S., 2000. Electrically controlled elasticity utilizing piezoelectric coupling. Journal of Applied Physics 87 (2), 863–868.
Edelman, S., Dereggi, A., 1976. Electroacoustic transducers with piezoelectric high polymer-films. Journal of the Audio Engineering Society 24 (7), 577–578.
Fiorillo, A.S., 1992. Design and characterisation of a PVDF ultrasonic range sensor. IEEE Transactions on Ultrasonics, Ferroelectrics and Frequency Control 39 (6), 688–692.
Fukada, E., Date, M., Kimura, K., Okubo, T., Kodama, H., Mokrý, P., Yamamoto, K., 2004. Sound isolation by piezoelectric polymer films connected to negative capacitance circuits. IEEE Transaction on Dielectric and Electrical Insulation 11 (2), 328–333.
Herbert, J.M., Wand, T.T., Glass, A.M., 1998. The Applications of Ferroelectric Polymers. Chapman & Hall.
ISO 10534-2:1998(E), 1998. Acoustics – Determination of sound absorption coefficient and impedance in impedance tubes – Part 2: Transfer-function method. ISO, Geneva, Switzerland.
Kodama, H., Okubo, T., Date, M., Fukada, E., 2002. In: Symposium on Rapid Prototyping Technologies-From Tissue Engineering to Conformal Electronics held at the 2001 MRS Fall Meeting, BOSTON, MA, NOV 28-30, 2001. Proceedings of Materials Research Society Symposium (Boston), vol. 698. Materials Research Society, 506 Keystone Drive, Warrendale, PA 15088-7563, USA, pp. 43–52.
Lerch, R., Sessler, G.M., 1980. Microphones with rigidly supported piezopolymer membranes. Journal of the Acoustical Society of America 67, 1379–1381.
Maddox, N., Plumblee, H., King, W., 1970. Frequency analysis of a cylindrically curved panel with clamped and elastic boundaries. Journal of Sound and Vibration 12 (2), 225–230. IN3, 231–249.
Mead, D., Bardell, N., 1986. Free vibration of a thin cylindrical shell with discrete axial stiffeners. Journal of Sound and Vibration 111 (2), 229–250.
Mokrý, P., Fukada, E., Yamamoto, K., 2003a. Noise shielding system utilizing a thin piezoelectric membrane and elasticity control. Journal of Applied Physics 94 (1), 789–796.
Mokrý, P., Fukada, E., Yamamoto, K., 2003b. Sound absorbing system as an application of the active elasticity control technique. Journal of Applied Physics 94 (11), 7356–7362.

Mustafa, B., Ali, R., 1987. Free vibration analysis of multi-symmetric stiffened shells. Computers & Structures 27 (6), 803–810.

Shen, P.-C., Chuang, D., 1990. Dynamic analysis of stiffened plates and shells using spline gauss collocation method. Computers & Structures 36 (4), 623–629.

Shen, P.-C., Wan, J.-G., 1987. Vibration analysis of flat shells by using *b* spline functions. Computers & Structures 25 (1), 1–10.

Sluka, T., Kodama, H., Fukada, E., Mokry, P., 2008. Sound shielding by a piezoelectric membrane and a negative capacitor with feedback control. IEEE Transactions on Ultrasonics, Ferroelectrics and Frequency Control 55 (8), 1859–1866.

Tamura, M., Yamaguchi, T., Oyabe, T., Yoshimi, T., 1975. Electroacoustic transducers with piezoelectric high polymer films. Journal of Audio Engineering Society 23 (1), 21–26.

Toda, M., Tosima, S., 2000. Theory of curved, clamped, piezoelectric film, air-borne transducers. IEEE Transactions on Ultrasonics, Ferroelectrics and Frequency Control 47 (6), 1421–1431.

Vinson, J.R., 1992. The Behavior of Shells Composed of Isotropic and Composite Materials (Solid Mechanics and Its Applications), 1st ed. Springer.

Wang, H., Toda, M., 1999. Curved pvdf air-borne transducer. IEEE Transactions on Ultrasonics, Ferroelectrics and Frequency Control 46 (6), 1375–1386.

Please cite this article in press as: Sluka, T., et al. A theory of sound transmission through a clamped curved piezoelectric membrane connected to a negative capacitor. Int. J. Solids Struct. (2010), doi:10.1016/j.ijsolstr.2010.04.019